THE JOURNAL OF PHYSICAL CHEMISTRY B

Article

pubs.acs.org/JPCB

# Molecular Origin of Piezo- and Pyroelectric Properties in Collagen Investigated by Molecular Dynamics Simulations

Harish Kumar Ravi, Fabio Simona, Jürg Hulliger,* and Michele Cascella*

Departement für Chemie und Biochemie, Universität Bern, Freiestrasse 3, 3012 Bern, Switzerland

Supporting Information

**ABSTRACT:** Molecular dynamics simulations were used to study the effect of mechanical and thermal stimuli on the electrostatic properties of collagen model helices. Our model sequences were based on glycine proline and hydroxyproline amino acids. We find that longitudinal mechanical strain induces significant variation of the polarization of the collagen fibril. Such a phenomenon is determined by reorientation of the backbone polar groups, which are free to respond to the mechanical solicitation. This non-negligible effect is facilitated by the peculiar folding structure of the collagen helix, which is characterized by the absence of an extended hydrogen-bond network. The stretching/compression of the helix requires a concomitant winding/unwinding motion of the global structure; therefore, the shear components of the stress tensor are the components that most effectively induce structural modification associated to the piezoelectric response. The present calculations also report a pyroelectric response to thermal activation. Model calculations indicate that the pyroelectric effect is dominated by secondary components associated with the piezoelectric tensor.

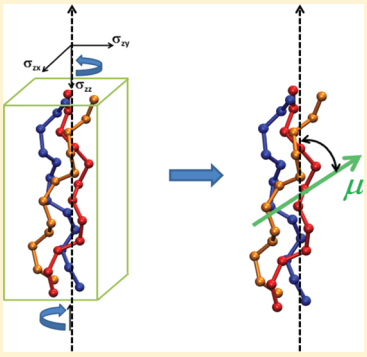


## 1. INTRODUCTION

Collagen belongs to the family of structural proteins that make up connective tissues such as bone, skin, and cartilage.[1,2] At the molecular level, the characteristic features of collagen fibrils are their long triple helical structure, about 300 nm long. The presence of the smallest amino acid glycine, in every third residue of the collagen protein, ensures that the three chains wind correctly to the characteristic triple helix. In fact, the collagen molecule is composed mostly of repeating amino acids of glycine-Xaa-Yaa, in which Xaa and Yaa can be any amino acid but are frequently either the amino acid proline (Pro) or its hydroxyproline (Hyp) variant.

Biological materials like collagen are found to exhibit partial polar alignment of molecular dipoles in their structure and such materials show piezoelectricity (variation of the macroscopic polarization upon mechanical strain) and pyroelectricity (variation of polarization upon temperature change).[3] These are among the fundamental properties of connective tissues reported for bones, teeth, vertebrate tendons,[4] blood vessels, intestines, and trachea[5] and also in plants.[6] Tissue polarity enables sensory receptors of complex organisms to detect mechanical and thermal stimuli from their environment.[7] Bassett and Becker discovered that the polar state is closely associated to the growth and remodeling of tissues such as bones.[8] Hearing is also associated with the piezoelectric properties of biopolymers.[9] Earlier studies on collagen fibrils suggested that there is a permanent electric moment in the direction of the longitudinal collagen axis with the polarity caused by the presence of large number of charged amino acids.[4] Shamos and Lavine speculated that the piezoelectricity apparently stems from a shearing stress, the actual effect being a displacement of charge due to the distortion of cross-linkages in the molecular structure, probably hydrogen bonds.[10] Other studies on collagen indicated an increase in the pyroelectric coefficient when increasing the negative charges in collagen molecule.[11] However, the electromechanical and thermal effects are not yet understood at an atomistic level.

In this work, we use molecular dynamics simulations to investigate the electrostatic response of model collagen proteins to both mechanical and thermal stimuli. In particular, we consider model collagen peptides formed by different repeating units of mixed glycine, proline and hydroxyproline amino acid sequences. This enables the study of shorter models instead of the entire molecule. In fact most progress to date, experimental or computational, has been made through the study of short collagen-like peptides.[12] The triple helical stability in collagen was studied by Stultz[13] et al. by molecular dynamics (MD) simulations. The mechanical properties of physiological and pathological models of collagen peptides were also investigated via steered MD simulations.[14] In addition the stability of collagen-like peptides[15] as a function of length has been investigated. A new parameters set for hydroxyprolines was developed that reproduces its preferential puckered conformation.[16] *Osteogenesis imperfecta*, a genetic disorder caused by mutations on collagen, was also previously investigated using MD simulations by Klein et al.[17−20] In this article, we examine the effects of induced stress and temperature on three collagen-like peptides, $[(\text{Gly-Pro-Pro})_7]_3$, $[\text{Gly-Pro-Pro})_3\text{-Gly-Hyp-Hyp-}$

**Received:** September 1, 2011
**Revised:** January 13, 2012
**Published:** January 13, 2012

$(Gly\text{-}Pro\text{-}Pro)_3]_3$ and $[(Gly\text{-}Pro\text{-}Hyp)_7]_3$, respectively, using MD simulations. For the helices we assume $C_3$ point symmetry, being spontaneously retained under the stress conditions applied. Under these symmetry conditions the piezoelectric tensor is of the form[21]

$$\begin{pmatrix} d_{11} & -d_{11} & 0 & d_{14} & d_{15} & -2d_{22} \\ -d_{22} & d_{22} & 0 & d_{15} & -d_{14} & -2d_{11} \\ d_{31} & d_{31} & d_{33} & 0 & 0 & 0 \end{pmatrix}$$

However, in tissues the symmetry can reduce to ∞2 (acentric) or ∞ (polar), featuring shear (∞2) and longitudinal components along the fiber assembly axis (∞).[22] The pyroelectric effect in $C_3$ shows a single component $p_3$ along the axis of the helical structure.

Calculations predict an increase in the longitudinal polarization of collagen upon compression (as opposed to a stretching) stress, induced by reorientation of the backbone polar groups. The same phenomenon was also studied by our model at different raising temperatures. We observe an increase of longitudinal polarization when temperature rises from 300 to 320 K, suggesting the presence of a positive pyroelectric effect when the fibril is not allowed to expand. Simulations, however, report no significant variations in the orientation distributions of polar groups when temperature rises further up to 340 K. Further heating results in partial unfolding of the structures.

## 2. THEORETICAL METHODS

The collagen protein was represented by a model where each chain of the collagen triple helix is composed of seven repeats of glycine and two proline residues $[(GPP)_7]_3$ (**GPP** model). In naturally occurring collagen, hydroxyprolines (abbreviated as O herafter) are present in significant abudance. In order to check the influence of hydroxylation on the properties of interest (piezo- and pyroelectricity), we constructed a second model, where the proline amino acids of the fourth repeat are substituted by hydroxyprolines $[(GPP)_3\text{-}GOO\text{-}(GPP)_3]_3$ (**GOO** model). A third model, where alternated proline and hydroxyproline sequences are present $[(GPO)_7]_3$ (**GPO** model) was also constructed. The **GPP** and **GOO** models constitute two limit cases, where consecutive PP or OO residues are present. The **GPO** model instead is a prototypic model of a sequence of biological significance. For each system, two independent sets of simulations were performed, one where the standard zwitterionic charges were present at the N- and C- termini and one where acetyl and *N*-methylamine groups were used to cap the N and C ends, respectively. A total of six models were simulated. The initial geometries of the **GPP** and **GOO** models were built starting from the deposited 1K6F[23] and 3A08[24] PDB structures respectively. The structure of the **GPO** model was built by molecular replacement from a relaxed structure of the **GOO** model. The missing hydrogen atoms were added using the default protonation of the structures by the xleap module in the Amber10 package.[25] The amber force field (FF99SB[26]) was used. The charges for the hydroxyprolines were obtained using a standard RESP procedure[27] (see the Supporting Information (SI)). The collagen models were solvated by 23 931 water molecules, and placed in a 80 × 80 × 135 Å$^3$ periodic box. The TIP3P[28] water model was used. The whole system was composed of 72 570 atoms. Particle Mesh Ewald routines were used to treat long-range electrostatic interactions.[29,30] A cutoff of 12 Å was used for the van der Waals interactions and the real part of the electrostatic interactions. The simulations were performed in the NpT ensemble with a Langevin chain of thermostats.[31] Bonds comprising hydrogen atoms were constrained with the SHAKE constraint algorithm[32] for the protein and the SETTLE algorithm[33]for the water. All simulations were performed using the NAMD program[34] and the trajectories were analyzed using the Gromacs[35] package.

First, energy minimization on the solvent was carried out, while holding the protein fixed, using the steepest descent algorithm for the first 300 steps followed by the conjugate gradient algorithm for 7200 steps. Then the same minimization cycles were repeated for the whole system. The energy minimized structures were heated up from 10 to 300 K in 0.3 ns MD, using a time step of 1.5 fs. The whole system was then equilibrated for 10 ns at 300 K.

**2.1. Simulations under Physical or Thermal Influence.** *Mechanical Strain.* The length of our collagen model was defined as the distance between the center of mass of the three Cα's at the N-termini and the center of mass of the three Cα's at the C-termini of the peptide chains. Unrestrained geometries have an average length of 58 Å. Physical strain on our collagen model was produced by applying harmonic restraints to the length of the model collagens. Specifically, a harmonic potential of spring constant 10 kcal/mol/Å$^2$ was used. The harmonic restraint was applied first to the natural equilibrium distance, which was progressively modified so to produce a compression and stretching of the collagen helix of about 3.5%, 7%, and 10.5% of its original length. Another spring constant of 2000 kcal/mol/degree$^2$ was applied to keep the orientation of the model fixed. The desired levels of compression and stretching were achieved in a 1.0 ns long simulation, and then kept for a production run of 10 ns.

*Thermal Effect.* By an independent set of simulations, the collagen model (kept at different compression/stretching conditions) was heated up to temperatures of 320, 340, and 360 K, respectively. The new temperatures were reached using simulated annealing protocols in about 3 ns, after thermalization, production runs of 10 ns simulations were performed.

## 3. RESULTS

For each condition tested (compression/stretching and heating) the same behavior was observed in all of our models. Also, the presence of the capping groups at the ends of the sequences did not affect the results found, which, within statistical uncertainty, remained the same. Therefore, in this results section, we present data referring to **GOO** with the capping groups at its termini only. Hereafter any reference to the **GOO** collagen model explicitly means the **GOO**-capped system.

In the **GOO** model of collagen, each Gly-Pro/Hyp-Pro/Hyp repeat unit presents three moieties to which a permanent electrostatic dipole can be associated. The three moieties are the Pro/Hyp-Gly peptide bond, the X-Pro/Hyp peptide bond (where X is either Gly or (Pro/Hyp), and the hydroxyl group present at the side-chain of hydroxyprolines (see Figure 1). The relative orientation of all permanent dipoles with respect to the longitudinal $C_3$ axis of the collagen helix was monitored along 10 ns of molecular dynamics simulation. In particular, we reported the statistical distributions of $\cos\theta = \mu_z/\mu$, where $\theta$ is the angle between the electrostatic dipole associated to any dipolar moiety present in our model, and the longitudinal $z$ axis of the collagen helix. This analysis was performed for the

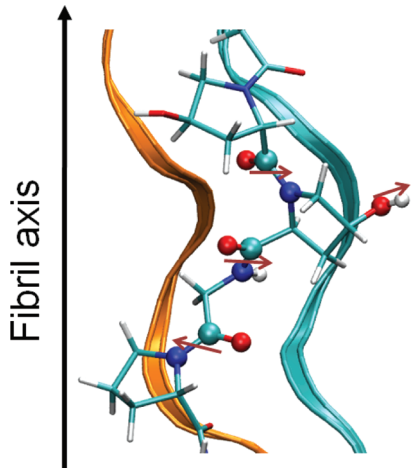


**Figure 1.** Structure of **GOO** collagen model. Zoomed view of the fibril structure. One amino acid sequence is represented in licorice. The other two filaments are depicted as ribbons for simplicity. The polar groups present in a triplet are shown in balls-and-sticks representation. The permanent electrostatic dipoles are represented by red arrows.

unperturbed, stretched, compressed and heated systems. The relaxed structure of collagen shows a static longitudinal polarization, mostly determined by Pro/Hyp-Gly peptide bond (Table 1). Due to the $C_3$ symmetry of the collagen triple helix, there is no transversal component of the permanent electrostatic dipole.

**Table 1. Average Longitudinal Component of the Electrostatic Dipole per GOO Triplet at Different Temperatures and at Different Deformations**

| | component of the dipole $\mu$ along the helical axis [Debye] | | |
|---|---|---|---|
| relative deformation of collagen | 300 K | 320 K | 340 K |
| 10.5% | 0.956 | 0.982 | 0.948 |
| 7% | 0.895 | 0.909 | 0.871 |
| 3.5% | 0.991 | 0.954 | 0.995 |
| 0% | 0.994 | 1.014 | 1.020 |
| −3.5% | 1.008 | 1.036 | 1.027 |
| −7% | 1.027 | 1.042 | 1.045 |
| −10.5% | 1.044 | 1.039 | 1.056 |

**3.1. Simulations of Collagen Model under Mechanical Stress.** The equilibrated **GOO** model was compressed to different target lengths by applying harmonic restraints to its ends (see the Theoretical Methods section for details). Figure 2 reports the statistical distribution of the cos $\theta$ between the different permanent dipole vectors and the longitudinal axis of the collagen in the equilibrated structure and at different stress conditions. Specifically, we forced the system to be stretched or compressed by 2, 4, and 6 Å. These mechanical deformations correspond to stretching the fibril model by 3.5%, 7%, or 10.5% or compressing it by 3.5%, 7%, or 10.5% of its relative original length.

For nonperturbed systems, the longitudinal orientations of the polar groups in the backbone show a Gaussian distribution of the cos $\theta$-values centered between −0.3 and 0.3, (Figure 2A−C) consistent with reported NMR and X-ray experiments, and tissue extracted GPP-based collagen models.[36−38] On the contrary, the OH group present at the hydroxyproline side-chain shows a much broader distribution (Figure 2D), with non-negligible probability for all possible orientational values. The highest probability in this case is found for OH pointing toward the C-terminal direction, which is associated to natural anti- configuration of the respective C−O torsional angle. All these equilibrium distributions produce a non-negligible dipole moment, oriented along the N-to-C direction (Table 1).

Upon application of longitudinal strain, the distributions of the cos $\theta$ for the backbone polar moieties are significantly affected. In particular, upon stretching, the distributions become more peaked, while, upon compression, a significant broadening of the peaks occurs. Of particular interest is the Pro/Hyp-Gly peptide bond. In fact, the distribution of its longitudinal component is characterized by a macroscopic shift upon deformation of the fibril (Figure 2A). On the contrary, the distribution of the side-chain hydroxyl groups is not significantly affected by mechanical stress perturbation along the longitudinal axis of the fibril. This result is in agreement with the fact that, in our model, the OH groups remain fully solvated by surrounding water, and therefore are not sensitive to structural modifications of the backbone induced by the compression. The overall reorientation of the polar groups leads to a neat longitudinal polarization of the system, which is proportional to the magnitude of the applied deformation, as shown in Table 1. The induced polarization in the compressed structures has the same orientation of the intrinsic dipole present in the unperturbed structure, while in the stretched structures it points opposite to the intrinsic dipole. Compression of the fibril is thus associated to an overall increase of the polarity of the system, while stretching of the fibril is associated to an overall depolarization of the system.

**3.2. Thermal Effect on Structure and Polarization of the Model.** The statistical orientation of the polar groups at different deformations was monitored as the system was heated to different temperatures. Specifically, in addition to a reference temperature of 300 K, we repeated simulations at 320, 340, and 360 K. Figure 3 reports the statistical distribution of cos $\theta$ for the polar groups for different deformations of the **GOO** model at 320 and 340 K. The qualitative behavior of the distributions is very similar to those of the same system at 300 K. Nonetheless, integration of the distributions report quantitative variations on the overall mean value of the total polarization. In fact, the distributions obtained at higher temperatures report a global overpolarization of the fibril. For most of the deformation conditions, this corresponds to a static increase of the longitudinal electrostatic dipole (~0.02 D per GPP triplet unit), as presented in Table 1. On the contrary, in the regime of small deformations (±3.5%) at 320 K, our model registers a significant enhancement of the piezoelectric response, with values of the instantaneous (de)polarization upon stretching/compression significantly higher than those at 300 K. Consequently, the present model predicts that application of longitudinal compression strain at higher temperature produces a higher polarization response.

When the fibril is deformed by more than 10% of its original length, deviations from the general rule occur. This has to be attributed to larger deformations induced in the structure, which produce a nonlinear response in the polarization. Increasing the temperature to nonphysiological conditions (360 K) also leads to nonlinear behavior in the polarization induced by larger structural modification. In fact, in these temperature conditions our model shows a partial unfolding of the native collagen helix structure with the chains at the end of the N-terminus region starting to unwind, thereby disturbing


dx.doi.org/10.1021/jp208436j | J. Phys. Chem. B 2012, 116, 1901−1907

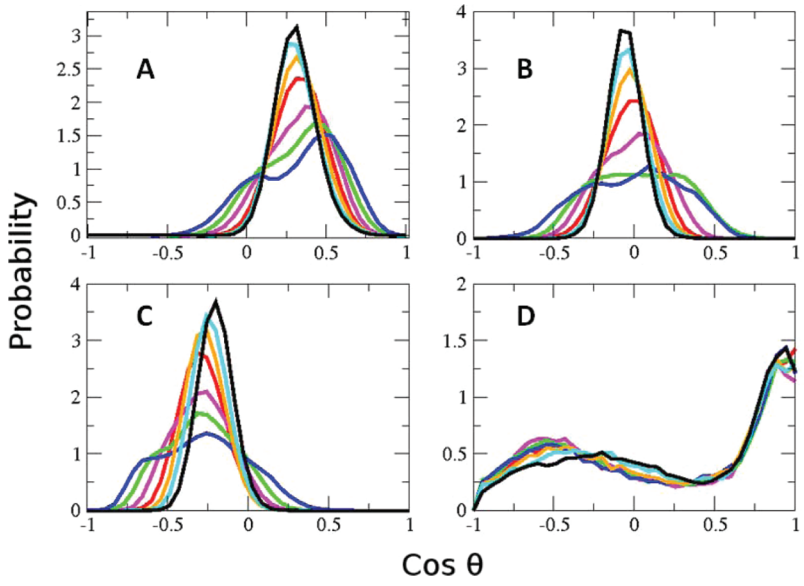


**Figure 2.** Variation in the cos $\theta$ distributions for different levels of mechanical stress. The line in red denotes the starting unstrained structure; deformations of the fibril length by 10.5% (black line), 7% (cyan), 3.5% (orange), −3.5% (magenta), −7% (green), and −10.5% (blue) relative to the original length are also shown. The four panels report cos $\theta$ distributions for (A) C═O groups of proline, (B) glycine, (C) the Pro/Hyp-Gly backbone group, and (D) the O−H group of hydroxyproline.

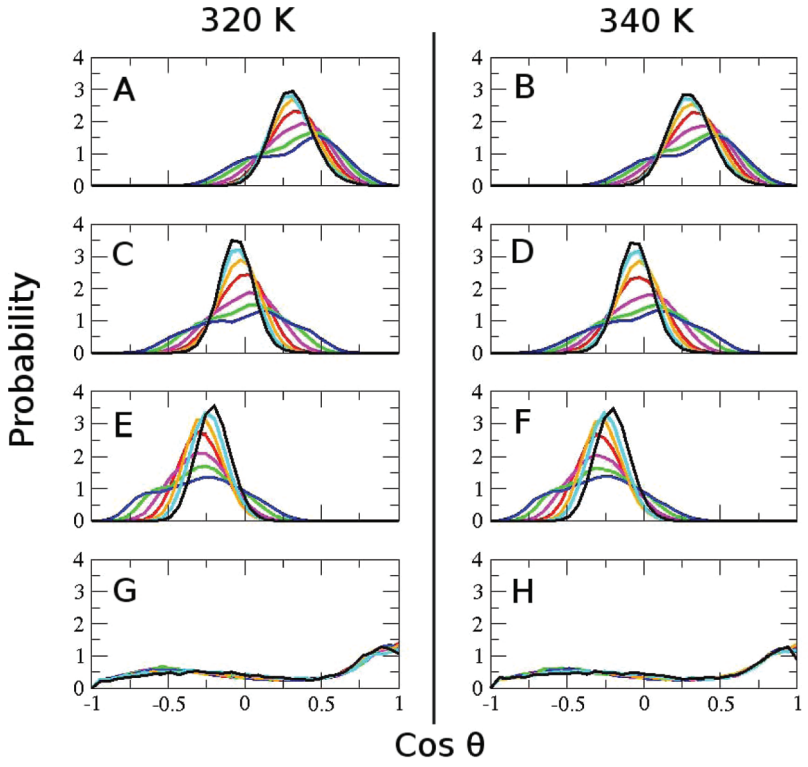


**Figure 3.** Variation in the cos $\theta$ distributions for different levels of mechanical stress at 320 and 340 K. The line in red denotes the starting unstrained structure. Relative stretchings of 10.5% (black line), 7% (cyan), 3.5% (orange), −3.5% (magenta), −7% (green), and −10.5% (blue) of the original length are reported. The panels report cos $\theta$ distributions at 320 and 340 K for (A and B) C═O groups of proline, (C and D) glycine, (E and F) the Pro/Hyp-Gly backbone group, and (G and H) the O−H group of hydroxyproline.

the symmetry of the triple helical nature of the collagen molecule (Figure 4).

*3.3. Stress and Structural Origin of the Induced Polarization.* Compression of the collagen model results in overall winding of the helical structure, while stretching of the collagen model results in unwinding of the helical structure. Specifically, simulations show a winding angle of 268° for the relaxed structure, which reaches 271° in the maximally compressed configuration, and drops to 266° in the maximally stretched configuration, respectively. The winding of the helix upon compression is a very general feature of rod-like bodies, which has been widely discussed in the literature.[39] At a molecular level, the winding motion is associated with a conformational change in the Ramachandran angles of the backbone peptides.


dx.doi.org/10.1021/jp208436j | J. Phys. Chem. B 2012, 116, 1901−1907

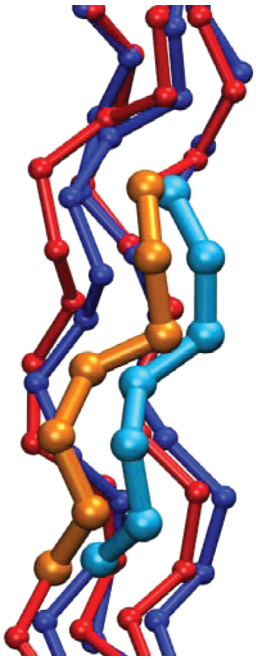

**Figure 4.** Superimposition of the structures of collagen models at 300 K (blue trace) and 360 K (red trace). The region where structural deformation in the helix core occurs, with consequent loss of the $C_3$ symmetry, is highlighted by orange and cyan colors.

These conformational changes are ultimately responsible for the reorientation of the polar groups present in the system and therefore, of the longitudinal polarization of the system. The winding motion implies a rotation of the ends of the helix on the plane perpendicular to the axis of the fibril (Figure 5);

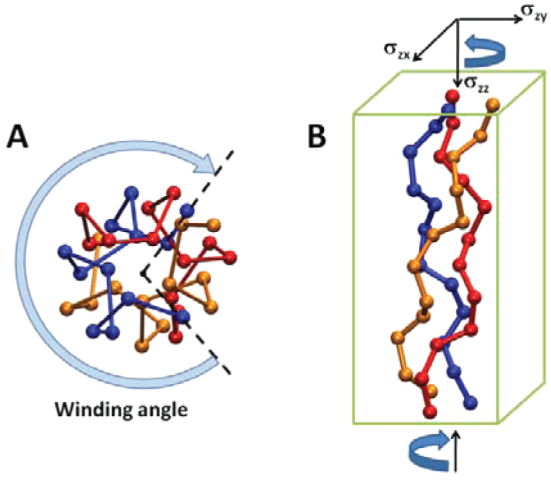


**Figure 5.** Molecular mechanism of fibril deformation. The longitudinal length of the collagen fibril is associated with its winding angle (panel A), which is determined by the Ramachandran torsional angles of the backbone of the amino acid chains. Any change in the winding angle by an external force is obtained by rotation of the ends of the collagen helix (panel B); thus, its modification is associated to the $\sigma_{zx}$ and $\sigma_{zy}$ shear components of the stress tensor.

therefore, it must be associated to the shear components of the stress tensor. Thus, the polarization measured in the present calculations can be attributed to large, positive values of the shear components of the piezoelectric tensor. The average bond length and bond angles present in the structure are not significantly affected by compression or stretching. Therefore, the torsional angles are the only degrees of freedom that are significantly responding to the imposed strain. This implies that a homogeneous deformation along the $z$ direction is not really occurring in our system and so the longitudinal components of the strain tensor only negligibly contribute to the phenomena mentioned above.

**3.4. Pyroelectricity: Thermal Expansion Coefficient and Elastic Constants.** The overall change in polarization upon heating can be understood by decomposing the pyroelectric effect into primary and secondary contributions. As thermal activation can affect expansion, the resultant change in length can induce a mechanical stress, which results in a change in polarization through the piezoelectric tensor. In summary, the total pyroelectric polarization $P_i$ along any component is given by[21]

$$P_i = P_i(\text{primary}) + \sum_{j,k,l,m=1}^{3} a_{ij} c_{jklm} d_{ilm} \Delta T$$

where $\alpha_{ij}$ is the thermal expansion, $c_{jklm}$ is the elastic stiffness, $d_{ilm}$ is the piezoelectric tensor, and $\Delta T$ is the increase in temperature. Our model predicts a qualitatively constant increase in the collagen polarization induced by an increase in temperature. When the fibril is restrained to its equilibrium length at 300 K, we find that the average force on the restraint slightly increases ($\Delta T > 0$, Figure 6); therefore, the fibril tends

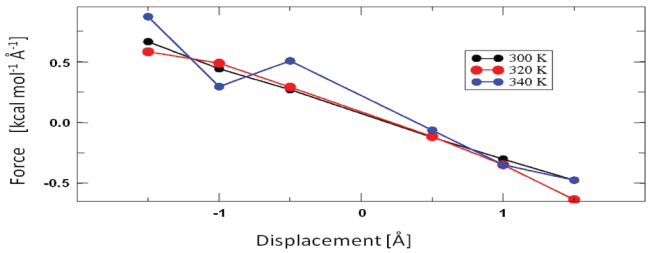


**Figure 6.** Collagen elasticity as a function of temperature. The average force required to induce small deformations of the collagen fibril is reported. The graph suggests a slight decrease of the elasticity between 300 and 320 K.

to expand (the longitudinal thermal expansion coefficient is positive). Despite the fact that the triple helical structure changes its length when heated to 320 K, (the lengths at 300 and 320 K remain within respective root-mean-square deviation), the collagen helix structure at 320 K is slightly more wound (~0.5°). Consequently, the orientation of the backbone polar moieties is more aligned to the longitudinal axis. This causes an overall increase in the total polarization under the condition of constant length. This evidence supports the idea that a non-negligible contribution to the pyroelectric effect comes from the secondary components associated to the piezoelectric tensor. Nonetheless, we stress here that our simulations, based on classical force fields, cannot account for other effects like thermal-induced anharmonic bond stretching and polarization, which could weigh for a correct estimate of the primary component of the pyroelectric effect.

The thermal response of the linear elasticity coefficient was monitored by estimating the force required to compress the system at different lengths for different temperatures. The results are shown in Figure 5. No significant variations in the


dx.doi.org/10.1021/jp208436j | J. Phys. Chem. B 2012, 116, 1901–1907

elasticity of the helix are observed when increasing the temperature from 300 to 320 K. At 340 K the thermal noise is too large to produce converged data within the simulation time.

## 4. DISCUSSION

Piezo- and pyroelectricity in collagen fibrils have been for many years associated to important biological phenomena like inflammatory response of connective tissues, directionality of bone growth, or muscular contraction. Our study shows how these properties are directly connected to the peculiar structure of the folding of the collagen helix. The supramolecular organization of the three amino acid chains is such that, unlike other folded structures, the polar backbone groups are not involved in strong interconnected hydrogen bond networks. Therefore, their orientation is extremely sensitive to any strain applied along the longitudinal direction of the helical structure. In fact, the mechanical response of our model to its longitudinal compression or stretching is associated to rotation of the dihedral backbone angles, which account for the global length of the helix. This motion would not be easily allowed in the presence of strong interconnected hydrogen bonded moieties, which would have been weakened by rotation of the corresponding polar groups. In fact, stretching of $\alpha$-helical or completely stretched peptides does not significantly affect their longitudinal macromolecular electrostatic dipole.[40] The possibility of easily changing relative orientations of its polar groups to adjust to mechanical strain makes the collagen-helix a very sensitive piezoelectric structure. The mechanism of piezoelectric response shown in our model is very general, and has to be associated to the global folding of the collagen structure. The mechanically induced electric response is related to the orientation of the backbone polar groups. Therefore, it is expected, on a qualitative basis, to be the same for any acid sequence folding in a collagen helix structure, and not only for our glycine-proline based model. On the other hand, the presence of other amino acids with bulkier side-chains can affect the relative stiffness of the helix, thus the intensity of the induced polarization may quantitatively vary from sequence to sequence. It must be said that in our calculations a fixed-charge force-field was used. Therefore, the quantitative data might be affected by such approximation, for example, by not taking in consideration the eventual (de)polarization of the bonds upon mechanical or thermal strain. In any case, we limited our study to a small perturbation regime only, where the global structure of the system remains substantially unaffected. Thus, we expect the eventual presence of these effects to be quantitatively negligible.

## 5. CONCLUSION

In essence, we conclude that collagen helices being the basic building blocks of large fibers in real tissue show a positive piezoelectric response ($\Delta P_3 > 0$) upon compressive stress. The effect originates from an enhanced winding of the helix. Increasing temperature in the range of about 20 K (system kept at constant length) a positive change in polarization is observed. As this response is associated with a slight increase in the degree of winding, we can say that the pyroelectric effect is of the secondary type. However, conditions in real tissues are different: upon heating, the assembly of fibers is most likely expanding. Thus individual helices are being stretched. This can produce a negative change in the total polarization, and thus a negative pyroelectric effect ($\Delta T > 0$, $\Delta P_3 < 0$) is expected for a comparison with experimental data. An experimental investigation along this line is in preparation.

## ■ ASSOCIATED CONTENT

### Ⓢ Supporting Information

RESP charges obtained for the hydroxyproline residue. This material is available free of charge via the Internet at http://pubs.acs.org.

## ■ AUTHOR INFORMATION

### Corresponding Author

*E-mail: juerg.hulliger@iac.unibe.ch; michele.cascella@iac.unibe.ch. Tel: + 41 31 631 4256. Fax: +41 31 631 3994.

### Notes

The authors declare no competing financial interest.

## ■ ACKNOWLEDGMENTS

The present research was supported by the Swiss National Science Foundation (Grant Nos. PP02_118930 and 200021_129472/1). We thank M. Burgener and Dr. G. Gannon for their critical reading of our manuscript.

## ■ REFERENCES

(1) Kielty, C. M.; Grant, M. E. In *Connective Tissue and its Heritable Disorders: Molecular, Genetic, and Medical Aspects*; Royce, P. M., Steinmann, B. U., Eds.; Wiley-Liss: New York, 2002.
(2) Prockop, D. J.; Kivirikko, K. I. *Annu. Rev. Biochem.* **1995**, *64*, 403−434.
(3) Goes, J. C.; Figueiro, S. D. *J. Mater. Sci. Lett.* **1999**, *18*, 983−986.
(4) Athenstaedt., H. *Nature* **1970**, *228*, 830−834.
(5) Fukada, E. *Biorheology* **1968**, *5*, 199−208.
(6) Simhon, M.; Athenstaedt, H. *Biophys. J.* **1980**, *29*, 331−337.
(7) Hulliger, J. *Biophys. J.* **2003**, *84*, 3501−3507.
(8) Basserr, C. A. L.; Pawluk, R. J.; Becker, R. O. *Nature* **1964**, *204*, 652.
(9) Fukada, E. *Ultrasonics* **1968**, *4*, 229−234.
(10) Shamos, M. H.; Lavin, L. S. *Nature* **1967**, *213*, 267−269.
(11) Goissis, G.; Piccirilli, L.; Goes, J. C.; Plepis, A. M. G.; Das-Gupta, D. K. *Artif. Organs* **2008**, *22*, 203−209.
(12) Sanghyun, P.; Klein, T. E.; Pande, V. S. *Biophys. J.* **2007**, *93*, 4108−4115.
(13) Gurry, T.; Nerenberg, P. S.; Stultz, C. M. *Biophys. J.* **2010**, *98*, 2634−2643.
(14) Gautieri, A.; Vesentini, S.; Montevecchi, F. M.; Redaelli, A. *J. Biomech.* **2008**, *41*, 3073−3077.
(15) Raman, S. S.; Parthasarathi, R.; Subramanian, V.; Ramasami, T. *J. Phys. Chem. B.* **2008**, *112*, 1533−1539.
(16) Sanghyun, P.; Radmer, R. J.; Klein, T. E.; Pande, V. S. *J. Comput. Chem.* **2005**, *26*, 1612−1616.
(17) Klein, T. E.; Huang, C. C. *Biopolymers* **1999**, *49*, 167−183.
(18) Mooney, S. D.; Huang, C. C.; Kollman, P. A.; Klein, T. E. *Biopolymers* **2001**, *58*, 347−353.
(19) Mooney, S. D.; Klein, T. E. *Mol. Cell. Proteomics* **2002**, *11*, 63−71.
(20) Radmer, R. J.; Klein, T. E. *Biochemistry* **2004**, *43*, 5314−23.
(21) Newnham, R. E. *Properties of Materials: Anisotropy, Symmetry, Structure*; Oxford University Press: Oxford, 2005.
(22) Lang, S. B. *Nature* **1966**, *21*, 704−705.
(23) Berisio, R.; Vitagliano, L.; Mazzarella, L.; Zagari, A. *Protein Sci.* **2002**, *11*, 262−270.
(24) Okuyama, K.; Morimoto, T.; Narita, H.; Kawaguchi, T.; Mizuno, K.; Bachinger, H. P.; Wu, G.; Noguchi, K. *Acta Crystallogr. .D* **2010**, *66*, 88−96.
(25) Case, D. A.; Darden, T. A.; Cheatham, T. E., III.; Simmerling, C. L.; Wang, J.; Duke, R. E.; Luo, R.; Crowley, M.; Walker, R. C.;

Zhang, W.; Merz, K. M.; Wang, B.; Hayik, S.; Roitberg, A.; Seabra, G.; Kolossváy, I.; Wong, K. F.; Paesani, F.; Vanicek, J.; Wu, X.; Brozell, S. R.; Steinbrecher, T.; Gohlke, H.; Yang, L.; Tan, C.; Mongan, J.; Hornak, V.; Cui, G.; Mathews, D. H.; Seetin, M. G.; Sagui, C.; Babin, V.; Kollman, P. A. *AMBER 10*; University of California, San Francisco, 2008.
(26) Hornak, V.; Abel, R.; Okur, A.; Strockbine, B.; Roitberg, A.; Simmerling, C. *Proteins* **2006**, *65*, 712−725.
(27) Dupradeau, F.-Y.; Pigache, A.; Zaffran, T.; Savineau, C.; Lelong, R.; Grivel, N.; Lelong, D.; Rosanski, W.; Cieplak, P. *Phys. Chem. Chem. Phys.* **2010**, *12*, 7821−7839.
(28) Jorgensen, W. L.; Chandrasekhar, J.; Madura, J. D.; Impey, R. W.; Klein, M. L. *J. Chem. Phys.* **1983**, *79*, 926−935.
(29) Darden, T.; York, D.; Pedersen, L. G. *J. Chem. Phys.* **1993**, *98*, 10089−10092.
(30) Essmann, U.; Perera, L.; Berkowitz, M. L.; Darden, T.; Lee, H.; Pedersen, L. G. *J. Chem. Phys.* **1995**, *103*, 8577−8593.
(31) Adelman, S. A.; Doll, J. D. *J. Chem. Phys.* **1976**, *64*, 2375−2388.
(32) Ryckaert, J.-P.; Ciccotti, G.; Berendsen, H. J .C. *J. Comput. Phys.* **1977**, *23*, 327−341.
(33) Miyamoto, S.; Kollman, P. A. *J. Comput. Chem.* **1992**, *13*, 952−962.
(34) Phillips, J. C.; Braun, R.; Wang, W.; Gumbart, J.; Tajkhorshid, E.; Villa, E.; Chipot, C.; Skeel, R. D.; Kale, L.; Schulten, K. *J. Comput. Chem.* **2005**, *26*, 1781−1802.
(35) Hess, B.; Kutzner, C.; Van der Spoel, D.; Lindahl, E. J. *J. Chem. Theory Comput.* **2008**, *4*, 435−447.
(36) Fechete, R.; Demco, D. E.; Blümich, B.; Eliav, U.; Navon, G. *J. Magn. Reson.* **2003**, *162*, 166−175.
(37) Fechete, R.; Demco, D. E.; Blümich, B. *NMR Biomed.* **2003**, *16*, 479−483.
(38) Falzon, G.; Pearson, S.; Murison, R. *Phys. Med. Biol.* **2008**, *53*, 6641−6652.
(39) Maritan, A.; Micheletti, C.; Trovato, A.; Banavar, J. R. *Nature* **2000**, *406*, 287−290.
(40) Cascella, M.; Neri, M. A.; Carloni, P.; Dal Peraro, M. *J. Chem. Theory Comput.* **2008**, *4*, 1378−1385.